

Interaction created effective flat bands in conducting polymers

Zsolt Gulácsi

Department of Theoretical Physics, University of Debrecen, H-4010 Debrecen, Hungary

(Dated: May 21, 2014)

Abstract

For a general class of conducting polymers with arbitrary large unit cell and different on-site Coulomb repulsion values on different type of sites, I demonstrate in exact terms the emergence possibility of an upper, interaction created “effective” flat band. This last appears as a consequence of a kinetic energy quench accompanied by a strong interaction energy decrease, and leads to a non-saturated ferromagnetic state. This ordered state clearly differs from the known flat-band ferromagnetism. This is because it emerges in a system without bare flat bands, requires inhomogeneous on-site Coulomb repulsions values, and possesses non-zero lower interaction limits at the emergence of the ordered phase.

I. INTRODUCTION

The band concept introduced by the band theory represents the foundation of our understanding of all solid state devices, and has been successfully used to explain main physical properties of solids. In its original form, the band structure theory assumes an infinite and homogeneous system in which the carriers, without experiencing inter-electronic interactions, but under the action of a periodic potential, attain their one-particle quantum mechanical $E_n(\mathbf{k})$ energy. This last defines the bare band structure described by the band index n and wave vector \mathbf{k} . The bare bands are in fact eigenstates of the non-interacting part of the Hamiltonian \hat{H}_0 . However, the above assumptions are broken in several practical situations, for example – neglecting surfaces, interfaces, inhomogeneities –, when inter-electronic interactions become important, e.g. in the case of strongly correlated systems. In such cases, the materials under consideration, simply cannot be understood in terms of the bare band structure. This is the reason why, the effects of the inter-electronic interactions, as a necessity, have been introduced in the calculation of electronic bands in different ways, especially based on the density functional theory (DFT). DFT tries to coopt the electron-electron many-body effects by the introduction of the exchange-correlation term in the functional of the electronic density. On its turn, the exchange correlation functional can be approximated in different ways, for example by local density approximation (LDA)¹, unrestricted Hartree-Fock treatment for the localized orbitals (LDA+U)², Green function techniques by approximating the self energy as a product between the Green's function G and a screened interaction contribution W (GW approximation)³, generalized gradient approximation (GGA)¹ which goes beyond LDA by taking account of the gradient corrections to the density, etc. For strongly correlated systems the DFT methods need to consider the interaction contributions more and more accurately, hence in this case there are also present special methods, as for example those which take into account input DFT data in dynamical mean-field treatment (DFT+DMFT)^{4,5}. For such systems is known that tending to exactitude, as for example in EXX method⁶ taking into account exact-exchange, the accuracy of the deduced result increases.

Besides the approximations presented above in a non-exclusive enumeration, there are rare cases when the effects of the interaction on the bare band structure can be exactly seen. For example, in integrable case, the Lieb and Wu solution⁷ shows that for 1D itinerant

and periodic systems with nearest neighbor hoppings and on-site Coulomb repulsion U , for any $U > 0$, Mott gap is present in the spectrum in exact terms, i.e. the “effective band” is always gaped in this case. In my knowledge, such exact results for non-integrable cases presently are not known. Starting from this observation, based on the aim to provide valuable information for non-integrable systems in this field, I present in this paper in exact terms how U creates an effective flat band in a system with completely dispersive bare bands, what is the physical reason of this process, and what type of consequences emerge. I note that the effect is important because information related to flat bands are representing a real driving force since they appear in a broad class of subjects of large interest today, as quantum Hall effect⁸, spin-quantum Hall effect⁹, topological phases^{9,10}, bose condensations¹¹, highly frustrated systems¹², delocalization effects¹³ or symmetry broken ordered phases¹⁴.

However the effect I describe is not exclusively restricted to quasi 1D systems (see the end of Sect.IV), the demonstration, born from properties observed in pentagon chain case^{15,16}, is presented on conducting polymers with arbitrary large unit cell containing a closed polygon and side groups. Conducting polymers are an important class of organic systems with a broad application potential at the level of nanodevices in electronics¹⁷ or medicine¹⁸. These materials are in fact conjugated polymers^{19,20}, which, being metallic, are intensively analyzed driven by the aim to produce different known phases emerging in metals at the level of plastic materials. The search for plastic ferromagnetism made entirely from nonmagnetic elements^{21–23} enrolls as well in this intensively studied research direction¹⁶. Concerning the theoretical interpretations, in the past, in such systems the inter-electronic interactions were not considered essential²⁴. However, in recent years, it becomes clear that in conducting and periodic organic systems, the Coulomb interaction between the carriers plays an important role. For example, the on-site Coulomb repulsion may even reach 10 eV²⁵, and it was also conjectured that in the highly doped region, the Coulomb interaction would be able to stabilize magnetic order²⁶, all this information being considered during theoretical studies^{15,16,27–34}.

The high Hubbard repulsion U values always lead to interesting physical consequences^{7,35–37}, so the study of these cases merits special attention. Hence, in order to consider in the present case properly the inter-electronic interaction and to account accurately for the correlation effects, we will use here exact methods. Since conducting polymers are non-integrable systems, the applied technique is special, and will be shortly presented below.

The method we use has no connections to Bethe ansatz, and is based on positive semidefinite operator properties. The procedure allows the non-approximated deduction of the multi-electronic, even particle number dependent ground states, and the non-approximated study of the low lying part of the excitation spectrum. The method is applicable for quantum mechanical interacting many-body systems, being independent on dimensionality and integrability. The technique first transforms in exact terms the system Hamiltonian (\hat{H}) in a positive semidefinite form $\hat{H} = \hat{P} + C_g$, where \hat{P} is a positive semidefinite operator, while C_g a scalar. For this step usually block operators ($\hat{A}_{\mathbf{i},\sigma}$) are used which represent a linear combination of canonical Fermi operators acting on the sites of finite blocks connected to the lattice site \mathbf{i} , the positive semidefinite form being preserved by the $\hat{A}_{\mathbf{i},\sigma}^\dagger \hat{A}_{\mathbf{i},\sigma}$ type of expressions. I note, that especially in the above system half filling concentration region, in treating the Hubbard type of interaction terms, positive semidefinite operators of the form $\hat{P}_{\mathbf{i}} = \hat{n}_{\mathbf{i},\uparrow} \hat{n}_{\mathbf{i},\downarrow} - (\hat{n}_{\mathbf{i},\uparrow} + \hat{n}_{\mathbf{i},\downarrow}) - 1$ are also used, which require at least one electron on the site \mathbf{i} for their zero minimum eigenvalue.

The transformation $\hat{H} = \hat{P} + C_g$ is valid when a specific relationship – called matching equations – is present connecting the \hat{H} , and block operator parameters (i.e. the numerical prefactors of the linear combination present in $\hat{A}_{\mathbf{i},\sigma}$). The matching equations, representing a coupled non-linear complex algebraic system of equations, must be solved first. The solution provides the expression of block operator coefficients and the scalar C_g in function of \hat{H} parameters, and, the parameter space region \mathcal{D} , where the transformation in positive semidefinite form of \hat{H} is valid. After this step, the exact ground state is constructed by deducing the most general wave vector $|u\rangle$ which satisfies the equation $\hat{P}|u\rangle = 0$. The procedure merits attention since several techniques for solving this last equation are available today^{15,16,39–41}. In the third step, the uniqueness of the solution is demonstrated by concentrating on the kernel $Ker(\hat{P})$ of the operator \hat{P} , [$Ker(\hat{P})$ is a Hilbert subspace containing all vectors $|v\rangle$ with the property $\hat{P}|v\rangle = 0$]. This is done by showing that i) $|u\rangle$ is placed inside $Ker(\hat{P})$, and ii) all components of $Ker(\hat{P})$ can be expressed in terms of $|u\rangle$. The uniqueness proof works in the degenerate case as well, when $\hat{P}|u(m)\rangle = 0$ holds, m is a degeneracy index, and $|u(m_1)\rangle$ and $|u(m_2)\rangle$, in the case of $m_1 \neq m_2$, are linearly independent. In this situation, for the uniqueness proof, we must demonstrate that i) $|u(m)\rangle$ is inside of $Ker(\hat{P})$ for all m values, and ii) all components of $Ker(\hat{P})$ can be expressed as linear combinations of $|u(m)\rangle$.

The last step of the method deduces the physical properties of the ground state by calculating different relevant and elevated ground state expectation values. We note that if the ground state $|\Psi_g\rangle = |u\rangle$, has been obtained, the corresponding ground state energy becomes $E_g = C_g$. I must underline, that if the ground state and ground state energy can be deduced as function of the total number of particles N (N is maintained constant during the calculation), we can derive as well non-approximated results relating the low lying part of the excitation spectrum via the particle number dependent chemical potential $\mu(N) = E(N) - E(N - 1)$. This can be done for example by deducing the charge gap $g = \delta\mu = \mu(N + 1) - \mu(N)$, where $g = 0$ ($g \neq 0$) reflects conducting (insulating) behavior.

I note that the transformation in positive semidefinite form of the Hamiltonian is always possible. This is because Hamiltonians describing physical systems have always a spectrum bounded below. If the lower bound of the spectrum is denoted by C_g , then $\hat{H} - C_g = \hat{P}$ is a positive semidefinite operator, independent on dimensionality and integrability. Since C_g becomes the ground state energy at the end of the calculations, it is important to note that when the transformation is performed, the explicit form of this constant in function of Hamiltonian parameters is not known [see Eq.(5)], hence the technique not requires the *a priori* knowledge of the ground state energy. Furthermore, the starting point of the method is a fixed Hamiltonian, hence pre-conceptions or starting information relating the ground state wave function are not used or needed. This is why, in the last step of the procedure, the physical properties of $|\Psi_g\rangle$ must be separately analyzed.

The above presented technique has allowed to deduce results in circumstances unimaginable before in the context of exact solutions as: periodic Anderson model in one⁴², two⁴³, or three^{38,39} dimensions; disordered and interacting systems in two dimensions⁴⁴; emergence of stripes and droplets in 2D⁴⁵; delocalization effect caused by the on-site Coulomb interaction in 2D¹³; non-Fermi liquid behavior in 3D³⁹; study of non-integrable quadrilateral^{40,41} or pentagon^{15,16} chains.

In the present paper, using the technique described above for general chain structures, first I rigorously demonstrate the emergence of an effective interaction created flat band, although the system possesses only dispersive bare bands. By analyzing the consequences, I show that in the studied parameter space region, ferromagnetism appears in this class of materials. The emergence of the ordered phase is entirely driven by a huge decrease of the interaction energy, which is accompanied by a quench of the kinetic energy. The kinetic

energy quench, is the physical reason for the appearance of the effective upper flat band, whose presence is demonstrated on quite general grounds in the general case. The effect is related to the presence of different U_i on-site Coulomb repulsion values at different type of sites inside the unit cell. This allows a redistribution of the double occupancy d_i at different type of sites, such to attain small d_i where U_i is high, and vice verse (i.e. by minimizing $\sum_i U_i d_i$ for fixed and given U_i and N values), leading to the observed huge interaction energy decrease possibility. When U_i is homogeneous, the described effect disappears. I note that in the presented case, a ferromagnetic state appears on the effective flat band, which differs significantly from the standard flat band ferromagnetism¹⁴ because: i) emerges in a system without bare flat bands, ii) requires inhomogeneous on-site Coulomb repulsion values, and iii) possesses non-zero lower limits for the interaction when the ordered phase appears.

The remaining part of the paper is structured as follows: Section II. presents the considered chain structures, Section III. transforms the Hamiltonian in positive semidefinite form, presents and solves the matching equations in the most general case. Section IV demonstrates that in the parameter space region where the transformation of the Hamiltonian in positive semidefinite form is possible to be done, an effective (i.e. interaction created) upper flat band emerges in the spectrum. Section V. describes the ground state obtained from the positive semidefinite form of the Hamiltonian, while Section VI. presents the physical properties of the ground state, and the physical characteristics present at the emergence of the ordered state. Finally, Section VII. containing the summary and conclusions, closes the presentation.

II. THE CHAIN STRUCTURES UNDER CONSIDERATION

One analyzes below a general polymer chain whose unit cell is schematically presented in Fig.1. It contains $m = m_p + m_e$ sites, from which m_p sites are present in a closed polygon, m_e sites are external sites connected to the polygon, and one has $m > 2$. The in-cell numbering of the sites is given by the index $n = 1, 2, \dots, m$, and the site positions relative to the lattice site \mathbf{i} are given by \mathbf{r}_n .

The Hamiltonian of the system can be written as $\hat{H} = \hat{H}_0 + \hat{H}_U$, where

$$\begin{aligned}\hat{H}_0 &= \sum_{\mathbf{i}, \sigma} \left[\sum_{n, n', n > n'} (t_{n, n'} \hat{c}_{\mathbf{i}+\mathbf{r}_n, \sigma}^\dagger \hat{c}_{\mathbf{i}+\mathbf{r}_{n'}, \sigma} + H.c.) \right] + \sum_{n=1}^m \epsilon_n \hat{n}_{\mathbf{i}+\mathbf{r}_n, \sigma}, \\ \hat{H}_U &= \sum_{\mathbf{i}} \sum_{n=1}^m U_n \hat{n}_{\mathbf{i}+\mathbf{r}_n, \uparrow} \hat{n}_{\mathbf{i}+\mathbf{r}_n, \downarrow},\end{aligned}\tag{1}$$

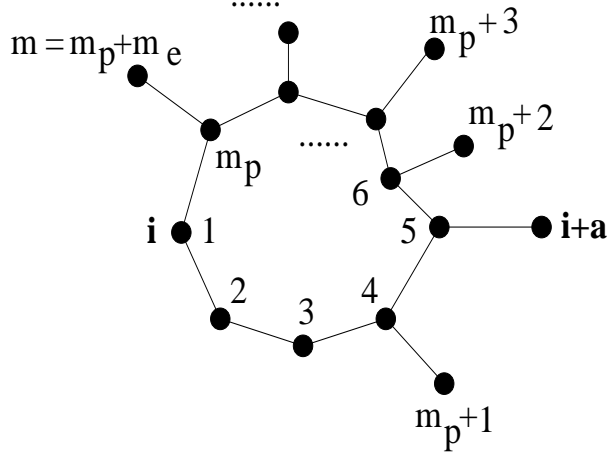


FIG. 1. The unit cell of the chain structures under consideration. The cell contains $m = m_p + m_e$ sites, where the m_p sites are included into a closed polygon, and m_e represents the number of external sites connected to the polygon. The unit cell is connected to the lattice site \mathbf{i} , while \mathbf{a} is the Bravais vector. The numbering of sites inside the unit cell is given by the index $n = 1, 2, \dots, m = m_p + m_e$. Sites $n = 1, 2, 3$ exemplifies sites without external links. The presence of such sites, or their placement, qualitatively not alters the obtained results.

where $\hat{c}_{\mathbf{j}, \sigma}^\dagger$ creates an electron with spin projection σ at the site \mathbf{j} , $\hat{n}_{\mathbf{j}, \sigma} = \hat{c}_{\mathbf{j}, \sigma}^\dagger \hat{c}_{\mathbf{j}, \sigma}$ represents the particle number operator for the spin projection σ at the site \mathbf{j} , $t_{n, n'}$ are nearest neighbor hopping matrix elements connecting the sites $\mathbf{i} + \mathbf{r}_{n'}$ and $\mathbf{i} + \mathbf{r}_n$, ϵ_n are on-site one-particle potentials at the site $\mathbf{i} + \mathbf{r}_n$, while $U_n > 0$ are on-site local Coulomb repulsion values. I note that during the calculation, periodic boundary conditions are used, and $\sum_{\mathbf{i}}, \prod_{\mathbf{i}}$, (or $\sum_{\mathbf{k}}, \prod_{\mathbf{k}}$ in momentum space) mean sums and products, respectively, over N_c cells. The number of sites in the system is denoted by $N_\Lambda = mN_c$, while the total number of electrons by $N \leq 2N_\Lambda$. The Hamiltonian parameters are arbitrary, but such chosen to not provide bare flat bands (i.e. \hat{H}_0 is without non-dispersive bands). Another important remark is related to the U_n Hubbard interaction values which depend on the particular environment and type of atom at a given site, hence are different on different type of sites inside the unit

cell. Particular cases of the general chain structure from Fig.1 are exemplified in Fig.2 for pentagon and hexagon cases.

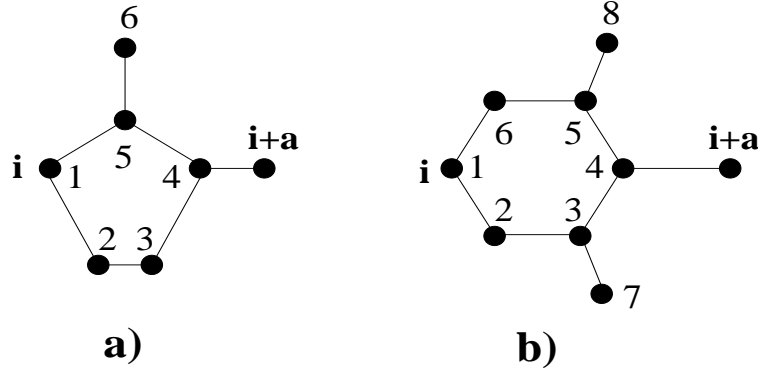


FIG. 2. Exemplifications of the general chain presented in Fig.1 for a) pentagon ($m_p = 5$, $m_e = 1$, $m = 6$), and b) hexagon ($m_p = 6$, $m_e = 2$, $m = 8$) cases. The unit cell connected to the lattice site \mathbf{i} shows the n index which provides the in-cell numbering of sites. \mathbf{a} represents the Bravais vector.

Concerning the contributions present in the Hamiltonian from (1), I note that i) the longer range Coulomb terms have been neglected because given by the many-body screening effects, these are much smaller than the on-site Coulomb repulsion, and ii) the electron-phonon contributions are not taken into consideration since they become important around half filling, while the results deduced in this paper are valid far away from half filling, in the strongly doped region.

III. THE TRANSFORMATION OF THE HAMILTONIAN IN POSITIVE SEMIDEFINITE FORM

A. The transcription of the Hamiltonian

For the transformation of the Hamiltonian we first introduce at each lattice site \mathbf{i} , $m - 1 = (m_p - 2) + (m_e + 1)$ blocks on which we define block operators as linear combinations of fermionic operators acting on the sites of the block. The $m - 1$ blocks are $m_p - 2$ triangles [namely the triangles constructed on the sites $(m_p, 1, 2)$, $(m_p, 2, 3)$, $(m_p, 3, 4)$, $(m_p, 4, 5)$, ..., (m_p, m_{p-1}, m_{p-2}) see Fig.1.], and $m_e + 1$ bonds [namely, in the case of the unit cell from Fig.1, the $m_e + 1$ bonds connecting the sites $(5, \mathbf{i} + \mathbf{a})$, $(4, m_p + 1)$, $(6, m_p + 2)$,

$(7, m_p + 3), \dots, (m_p, m_p + m_e)]$. Consequently, the introduced $m - 1$ block operators become

$$\begin{aligned}
\hat{G}_{\alpha, \mathbf{i}, \sigma}^\dagger &= a_{\alpha, m_p}^* \hat{c}_{\mathbf{i} + \mathbf{r}_{m_p}, \sigma}^\dagger + a_{\alpha, \alpha}^* \hat{c}_{\mathbf{i} + \mathbf{r}_\alpha, \sigma}^\dagger + a_{\alpha, \alpha+1}^* \hat{c}_{\mathbf{i} + \mathbf{r}_{\alpha+1}, \sigma}^\dagger, \\
\hat{G}_{m_p-1, \mathbf{i}, \sigma}^\dagger &= a_{m_p-1, 5}^* \hat{c}_{\mathbf{i} + \mathbf{r}_5, \sigma}^\dagger + a_{m_p-1, m+1}^* \hat{c}_{\mathbf{i} + \mathbf{a}, \sigma}^\dagger, \\
\hat{G}_{m_p, \mathbf{i}, \sigma}^\dagger &= a_{m_p, 4}^* \hat{c}_{\mathbf{i} + \mathbf{r}_4, \sigma}^\dagger + a_{m_p, m_p+1}^* \hat{c}_{\mathbf{i} + \mathbf{r}_{m_p+1}, \sigma}^\dagger, \\
\hat{G}_{m_p+\beta, \mathbf{i}, \sigma}^\dagger &= a_{m_p+\beta, \beta+5}^* \hat{c}_{\mathbf{i} + \mathbf{r}_{\beta+5}, \sigma}^\dagger + a_{m_p+\beta, m_p+\beta+1}^* \hat{c}_{\mathbf{i} + \mathbf{r}_{m_p+\beta+1}, \sigma}^\dagger,
\end{aligned} \tag{2}$$

where in the first row $\alpha = 1, 2, \dots, m_p - 2$ represents the index of the block operators constructed on triangles, the second and third line describes the first two block operators defined on bonds, namely those constructed on the site pairs $(4, m_p + 1)$, and $(5, \mathbf{i} + \mathbf{a})$, and finally, the last row with the index $\beta = 1, 2, \dots, m_e - 1$ presents the remaining block operators defined on bonds. Furthermore, in Eq.(2), the coefficients $a_{m, m'}^*$ are representing the numerical prefactors of the site $\mathbf{i} + \mathbf{r}_{m'}$ in the block operator $\hat{G}_{m, \mathbf{i}, \sigma}^\dagger$. I underline that if an external bond is missing from the polymer, then the corresponding block operator (on the respective bond) is also missing from Eq.(2).

Based on the fact that the block operators in Eq.(2) are defined in each unit cell, one constructs the positive semidefinite operator

$$\hat{P}_I = \sum_{\mathbf{i}, \sigma} \sum_{\gamma=1}^{m-1} \hat{G}_{\gamma, \mathbf{i}, \sigma} \hat{G}_{\gamma, \mathbf{i}, \sigma}^\dagger, \tag{3}$$

and introduce the positive semidefinite operator $\hat{P}_{\mathbf{j}} = \hat{n}_{\mathbf{j}, \uparrow} \hat{n}_{\mathbf{j}, \downarrow} - (\hat{n}_{\mathbf{j}, \uparrow} + \hat{n}_{\mathbf{j}, \downarrow}) + 1$, (see Sect.I) which gives rise to the positive semidefinite form

$$\hat{P}_{II} = \sum_{n=1}^m U_n \hat{P}_n, \quad \hat{P}_n = \sum_{\mathbf{i}} \hat{P}_{\mathbf{i} + \mathbf{r}_n}, \quad U_n > 0. \tag{4}$$

Using \hat{P}_I and \hat{P}_{II} , the transformed Hamiltonian becomes

$$\hat{H} = \hat{P}_I + \hat{P}_{II} + C_g, \tag{5}$$

where the scalar C_g has the expression $C_g = q_U N - N_c [\sum_{n=1}^m U_n + 2 \sum_{\gamma=1}^{m-1} q_\gamma]$. Furthermore, $q_\gamma = \{\hat{G}_{\gamma, \mathbf{i}, \sigma}, \hat{G}_{\gamma, \mathbf{i}, \sigma}^\dagger\}$, q_U is a scalar which depends on the parameters of \hat{H} , and can be obtained as a solution of the matching system of equations Eqs.(6-10). These reflect the fact that we transformed the starting \hat{H} from (1) dependent on the initial Hamiltonian parameters $t_{n, n'}, \epsilon_n, U_n$, into \hat{H} from (5) dependent on block operator parameters $a_{n, n'}$. Consequently, this transformation will be valid only if a relationship exists between block

operator parameters and the Hamiltonian parameters. This relationship is fixed by the matching equations which are obtained as follows: i) one effectuates the calculations in the right side of (5) obtaining the expression from (1), but with coefficients dependent on block operator parameters, and ii) taking equal the coefficients of the same operator in (1) and (5). The results are presented below.

B. The matching equations

The matching equations preserving the validity of the transformation of \hat{H} described above have the following structure for the general unit cell presented in Fig.1:

i) For the nearest neighbor bonds contained in the polygon and present in the Hamiltonian via the in-polygon nearest neighbor hopping matrix elements, one obtains

$$-t_{1,m_p} = a_{1,1}^* a_{1,m_p}, \quad -t_{m_p,m_p-1} = a_{m_p-2,m_p}^* a_{m_p-2,m_p-1}, \quad -t_{\alpha+1,\alpha} = a_{\alpha,\alpha+1}^* a_{\alpha,\alpha}, \quad (6)$$

where with $\alpha = 1, 2, \dots, m_p - 2$, one has in total m_p equations.

ii) For the bonds included in the triangular blocks used in the construction of the block operators, but with zero hopping matrix elements in the Hamiltonian from (1), one obtains $m_p - 3$ equations with $\alpha' = 1, 2, \dots, m_p - 3$:

$$a_{\alpha',\alpha'+1}^* a_{\alpha',m_p} + a_{\alpha'+1,\alpha'+1}^* a_{\alpha'+1,m_p} = t_{\alpha'+1,m_p} = 0. \quad (7)$$

iii) For the external bonds placed outside of the polygon one finds $m_e + 1$ equations

$$\begin{aligned} -t_{5,m+1} = -t_{\mathbf{i}+\mathbf{r}_5,\mathbf{i}+\mathbf{a}} &= a_{m_p-1,5}^* a_{m_p-1,m+1}, \quad -t_{4,m_p+1} = a_{m_p,4}^* a_{m_p,m_p+1}, \\ -t_{\alpha''+4,m_p+\alpha''} &= a_{m_p+\alpha''-1,\alpha''+4}^* a_{m_p+\alpha''-1,m_p+\alpha''}, \end{aligned} \quad (8)$$

where $\alpha'' = \beta + 1 = 2, 3, \dots, m_e$.

iv) For the on-site contributions of the sites placed inside the polygon one has m_p equations. Namely, by introducing $\bar{q}_U(n) = q_U - (U_n + \epsilon_n)$, one has

$$\begin{aligned} \bar{q}_U(1) &= |a_{1,1}|^2 + |a_{m_p-1,m+1}|^2, \quad \bar{q}_U(2) = |a_{1,2}|^2 + |a_{2,2}|^2, \quad \bar{q}_U(3) = |a_{2,3}|^2 + |a_{3,3}|^2, \\ \bar{q}_U(4) &= |a_{3,4}|^2 + |a_{4,4}|^2 + |a_{m_p,4}|^2, \quad \bar{q}_U(5) = |a_{4,5}|^2 + |a_{5,5}|^2 + |a_{m_p-1,5}|^2, \\ \bar{q}_U(n) &= |a_{n-1,n}|^2 + |a_{n,n}|^2 + |a_{m_p+n-5,n}|^2, \quad n = 6, 7, \dots, m_p - 2 \\ \bar{q}_U(m_p - 1) &= |a_{m_p-2,m_p-1}|^2 + |a_{m-2,m_p-1}|^2, \quad \bar{q}_U(m_p) = \sum_{\alpha=1}^{m_p-2} |a_{\alpha,m_p}|^2 + |a_{m-1,m_p}|^2. \end{aligned} \quad (9)$$

v) Finally, for the external sites placed outside of the polygon and representing side groups, with $\gamma = 1, 2, \dots, m_e$, one obtains m_e equations of the form

$$\bar{q}_U(m_p + \gamma) = |a_{m_p+\gamma-1, m_p+\gamma}|^2, \quad (10)$$

The equations Eqs.(6-10) are representing the matching system of equations, which contains $M_e = 3m_p + 2m_e - 2$ coupled, non-linear and complex algebraic equations. The unknown variables of this system of equations are the block operator coefficients and q_U , their number being $M_u = 3(m_p - 2) + 2(m_e + 1) + 1 = 3m_p + 2m_e - 3$. Since $M_e > M_u$, a supplementary equality remains between the parameters, which delimits a parameter space region \mathcal{D} where the transformation (5) is valid.

C. Solution of the matching equations

The solution technique for the matching equations Eqs.(6-10) for all m values is similar, and it has practically two steps: a) First the equations connected to hopping matrix elements are used to express unknown parameters (i.e. block operator coefficients $a_{n,n'}$) in function of other unknown parameters, strongly reducing in this manner the number of equations and unknown variables of the problem. b) The expressed variables are introduced in the remaining equations containing the U_n values. In the present case, for a) one uses Eqs.(8,10) in order to express all coefficients of the m_e block operators defined on bonds not touching the site $\mathbf{i} + \mathbf{a}$. Using the indices $\gamma = 1, 2, \dots, m_e$ and $\beta = 1, 2, \dots, m_e - 1$, one finds

$$\begin{aligned} a_{m_p+\gamma-1, m_p+\gamma} &= \sqrt{\bar{q}_U(m_p + \gamma)}, \quad a_{m_p+\beta, \beta+5} = -\frac{t_{\beta+1, m_p+\beta+1}}{\sqrt{\bar{q}_U(m_p + \beta + 1)}}, \\ a_{m_p, 4} &= -\frac{t_{4, m_p+1}}{\sqrt{\bar{q}_U(m_p + 1)}}, \quad a_{m_p-1, 5}^* = -\frac{t_{5, m+1}}{a_{m_p-1, m+1}}, \end{aligned} \quad (11)$$

where, supplementary, the last equation in the second row is obtained from the first equality of (8). Based on (11), one has $2m_e + 1$ unknown variables expressed. Now the equations Eqs.(6,7) are used in order to provide block operator parameters of the $m_p - 2$ block operators defined on triangles, as follows: For both $\hat{G}_{1, \mathbf{i}, \sigma}^\dagger$ and $\hat{G}_{m_p-2, \mathbf{i}, \sigma}^\dagger$ operators, two-two coefficients can be obtained from (6), namely

$$a_{1,2}^* = -\frac{t_{2,1}}{a_{1,1}}, a_{1, m_p}^* = -\frac{t_{1, m_p}}{a_{1,1}}, a_{m_p-2, m_p-1}^* = -\frac{t_{m_p-1, m_p-2}}{a_{m_p-2, m_p-2}}, a_{m_p-2, m_p}^* = \frac{t_{m_p, m_p-1}}{t_{m_p-1, m_p-2}} a_{m_p-2, m_p}^* \quad (12)$$

while for the remaining $m_p - 4$ triangles, again from (6), one coefficient per block operator can be expressed as ($n = 2, 3, \dots, m_p - 3$).

$$a_{n,n+1}^* = -\frac{t_{n+1,n}}{a_{n,n}}. \quad (13)$$

After this step, using (7), a second coefficient can be obtained for the block operators whose prefactors are present in (13), namely ($\alpha' = 1, 2, \dots, m_p - 3$):

$$a_{\alpha'+1,m_p} = -\frac{[\prod_{\alpha=1}^{\alpha'} t_{\alpha+1,\alpha}] t_{1,m_p}}{a_{\alpha'+1,\alpha'+1}^* [\prod_{\alpha=1}^{\alpha'} |a_{\alpha,\alpha}|^2]}. \quad (14)$$

Now it can be observed that the last (i.e $\alpha' = m_p - 3$) equation from (14), and the last equation from (12) express the same variable a_{m_p-2,m_p} , hence one finds

$$\prod_{\alpha=1}^{m_p-2} |a_{\alpha,\alpha}|^2 = -[\prod_{\alpha=1}^{m_p-2} t_{\alpha+1,\alpha}] \frac{t_{1,m_p}}{t_{m_p,m_p-1}}, \quad (15)$$

consequently, for the solution to exist one must have

$$[\prod_{\alpha=1}^{m_p-2} t_{\alpha+1,\alpha}] \frac{t_{1,m_p}}{t_{m_p,m_p-1}} < 0. \quad (16)$$

Equation (16) shows that solutions exist only if the product of all hopping matrix elements along the closed polygon is a negative number, and this result represents one of the conditions which defines \mathcal{D} .

In Eqs.(12-15), further $M_2 = 2m_p - 3$ coefficients are expressed, while in (11) $M_1 = 2m_e + 1$ coefficients are given, so one has up to this stage $M_1 + M_2 = 2m_p + 2m_e - 2$ unknown parameters given in function of other unknown parameters. Hence one remains with $M_u - (M_1 + M_2) = m_p - 1$ unknown variables (i.e. $a_{1,1}, a_{2,2}, \dots, a_{m_p-3,m_p-3}, a_{m_p-1,m+1}$ and q_U), and the remaining m_p matching equations from (9). The prefactor a_{m_p-2,m_p-2} could be expressed in principle from (15) (but see below).

Introducing all the obtained results in (9), the remaining m_p matching equations read

$$\begin{aligned}
\bar{q}_U(1) &= |a_{1,1}|^2 + |a_{m_p-1,m+1}|^2, \quad \bar{q}_U(2) = \frac{t_{2,1}^2}{|a_{1,1}|^2} + |a_{2,2}|^2, \quad \bar{q}_U(3) = \frac{t_{3,2}^2}{|a_{2,2}|^2} + |a_{3,3}|^2, \\
\bar{q}_U(4) &= \frac{t_{4,3}^2}{|a_{3,3}|^2} + |a_{4,4}|^2 + \frac{t_{4,m_p+1}^2}{\bar{q}_U(m_p+1)}, \quad \bar{q}_U(5) = \frac{t_{5,4}^2}{|a_{4,4}|^2} + |a_{5,5}|^2 + \frac{t_{5,m+1}^2}{|a_{m_p-1,m+1}|^2}, \\
\bar{q}_U(n) &= \frac{t_{n,n-1}^2}{|a_{n-1,n-1}|^2} + |a_{n,n}|^2 + \frac{t_{n,m_p+n-4}^2}{\bar{q}_U(m_p+n-4)}, \quad n = 6, 7, \dots, m_p-2, \\
\bar{q}_U(m_p-1) &= \frac{t_{m_p-1,m_p-2}^2}{|a_{m_p-2,m_p-2}|^2} + \frac{t_{m_p-1,m-1}^2}{\bar{q}_U(m-1)}, \\
q_U - (U_{m_p} + \epsilon_{m_p}) &= \sum_{\alpha=1}^{m_p-2} |a_{\alpha,m_p}|^2 + \frac{t_{m_p,m}^2}{q_U - (U_m + \epsilon_m)}, \tag{17}
\end{aligned}$$

where, in the last line, concerning $|a_{\alpha,m_p}|^2$, for $\alpha = 1$ it is taken from the second term of (12), while for $\alpha \geq 2$ from (14).

A simple procedure can be applied for solving (17). From the second line from the bottom $|a_{m_p-2,m_p-2}|^2$ can be expressed, then from the third line from the bottom $|a_{m_p-3,m_p-3}|^2$, similarly, from the fourth line from the bottom $|a_{m_p-4,m_p-4}|^2$, etc. Introducing all these results in the last line of (17) one obtains the equation for q_U . Eq.(15) remains a supplementary condition defining \mathcal{D} . Hence \mathcal{D} will be given by (15,16) and the conditions $q_U > U_\alpha + \epsilon_\alpha$, $\alpha = 1, 2, \dots, m_p$.

IV. THE EFFECTIVE UPPER FLAT BAND CREATED BY INTERACTION

In this section I show that the transformation of the Hamiltonian in positive semidefinite form (5) together with the solution of the matching equations presented in subsection III.C. describe in fact the emergence of an upper effective (i.e. interaction created) flat band.

Let us consider that we are placed inside \mathcal{D} in the parameter space. This means that the matching equations allow solution, consequently the operators $\hat{G}_{\alpha,i,\sigma}^\dagger$ exist, are well defined, and are U_n dependent as shown by the block operator coefficients expressed for example in (11,17). In these conditions \hat{P}_I from (3) entering in the Hamiltonian (5) exists and has U_n dependence through the $\hat{G}_{\alpha,i,\sigma}^\dagger$ operators. Furthermore, the unique one-particle (i.e. “kinetic”) contribution in (5) originates from \hat{P}_I via

$$\hat{P}_I = \hat{H}_{kin} + C_P, \quad \hat{H}_{kin} = - \sum_{i,\sigma} \sum_{\alpha=1}^{m-1} \hat{G}_{\alpha,i,\sigma}^\dagger \hat{G}_{\alpha,i,\sigma}, \quad C_P = 2N_c \sum_{\alpha=1}^{m-1} q_\alpha, \tag{18}$$

where C_p and q_α [defined under (5)], are numerical coefficients. Consequently the transformed Hamiltonian (5) becomes

$$\hat{H} = \hat{H}_{kin} + \hat{H}_{int} + C, \quad (19)$$

where for the interaction term one has $\hat{H}_{int} = \hat{P}_{II}$, and $C = C_p + C_g$ is a constant which shifts globally the energy. Since \hat{H}_{kin} is a one-particle term, it provides a band structure which is “effective” because was created by interaction (i.e. depends on the U_n interaction terms). In what will follows, we will be interested to see what are the characteristics of the effective band structure created by \hat{H}_{kin} .

Since m sites are present in the unit cell, and the σ index has two values, in \mathbf{r} -space one has $2mN_c$ different and linearly independent $\hat{c}_{n,\mathbf{i},\sigma}$, $n = 1, 2, \dots, m$ starting canonical Fermi operators constructing $\hat{G}_{\alpha,\mathbf{i},\sigma}^\dagger$. The $\hat{c}_{n,\mathbf{i},\sigma}$ operators transformed in \mathbf{k} -space provide also $2mN_c$ different and linearly independent $\hat{c}_{n,\mathbf{k},\sigma}$ canonical Fermi operators. Furthermore, one has m bands in the band structure, and each band accepts maximum $2N_c$ electrons.

Now one turns to \hat{H}_{kin} which contain $2N_c(m-1)$ fermionic operators $\hat{G}_{\alpha,\mathbf{i},\sigma}$, $\alpha = 1, 2, \dots, m-1$. Because an $\hat{G}_{\alpha,\mathbf{i},\sigma}$ operator, for an arbitrary $\alpha = n_1$, has at least one site not contained in all $\hat{G}_{\beta,\mathbf{i},\sigma}$ operators with $\beta < n_1$, the block operators $\hat{G}_{\alpha,\mathbf{i},\sigma}$ are linearly independent. Transforming them in \mathbf{k} -space, these operators lead to $2N_c(m-1)$ different and linearly independent $\hat{G}_{\alpha,\mathbf{k},\sigma}$ operators which however are not canonical (i.e. $q_\alpha \neq 1$, and evidently $q_\alpha \neq 0$). Because of this reason, by normalization to unity, we transform the $\hat{G}_{\alpha,\mathbf{k},\sigma}$ set into a normalized set obtaining $2N_c(m-1)$ canonical Fermi operators $\hat{C}_{\alpha,\mathbf{k},\sigma}$ (i.e. now, besides $\{\hat{C}_{\alpha,\mathbf{k},\sigma}, \hat{C}_{\alpha',\mathbf{k}',\sigma'}\} = 0$, $\{\hat{C}_{\alpha,\mathbf{k},\sigma}^\dagger, \hat{C}_{\alpha',\mathbf{k}',\sigma'}^\dagger\} = 0$, also $\{\hat{C}_{\alpha,\mathbf{k},\sigma}, \hat{C}_{\alpha',\mathbf{k}',\sigma'}^\dagger\} = \delta_{\alpha,\alpha'}\delta_{\sigma,\sigma'}\delta_{\mathbf{k},\mathbf{k}'}$ are satisfied). Please note that one has $2mN_c$ different starting operators $\hat{c}_{n,\mathbf{k},\sigma}$, but the existing $\hat{G}_{\alpha,\mathbf{k},\sigma}$ provide only $2N_c(m-1)$ different $\hat{C}_{\alpha,\mathbf{k},\sigma}$ operators, so at this stage $2N_c$ operators $\hat{C}_{\alpha,\mathbf{k},\sigma}$ are missing, namely those which correspond to $\alpha = m$.

Collecting all the presented information, one has for each $\alpha = 1, 2, \dots, m-1$ the expression

$$-\sum_{\mathbf{i},\sigma} \hat{G}_{\alpha,\mathbf{i},\sigma}^\dagger \hat{G}_{\alpha,\mathbf{i},\sigma} = \sum_{\mathbf{k},\sigma} \eta_\alpha(\mathbf{k}) \hat{C}_{\alpha,\mathbf{k},\sigma}^\dagger \hat{C}_{\alpha,\mathbf{k},\sigma}. \quad (20)$$

Since the left side of (20) is negative definite, and $\hat{C}_{\alpha,\mathbf{k},\sigma}$ are canonical Fermi operators, it results that $\eta_\alpha(\mathbf{k}) < 0$ for all \mathbf{k} and α . Indeed, if a state $|\alpha, \mathbf{k}, \sigma\rangle$ state exists with the property $\hat{C}_{\alpha',\mathbf{k}',\sigma'}^\dagger \hat{C}_{\alpha',\mathbf{k}',\sigma'} |\alpha, \mathbf{k}, \sigma\rangle = \delta_{\alpha',\alpha} \delta_{\mathbf{k}',\mathbf{k}} \delta_{\sigma',\sigma} |\alpha, \mathbf{k}, \sigma\rangle$ and $\eta_\alpha(\mathbf{k}) \geq 0$, this would contradict the

negative definite nature of the left side of (20). Consequently, \hat{H}_{kin} becomes

$$\hat{H}_{kin} = \sum_{\mathbf{k}, \sigma} \sum_{\alpha=1}^{m-1} \eta_{\alpha}(\mathbf{k}) \hat{C}_{\alpha, \mathbf{k}, \sigma}^{\dagger} \hat{C}_{\alpha, \mathbf{k}, \sigma} \quad (21)$$

Eq.(21) describes $m - 1$ effective (interaction dependent) bands placed at negative energy values, and $\hat{C}_{\alpha, \mathbf{k}, \sigma}^{\dagger}$ creates an electron with spin σ in the α th effective band.

Now three steps follow: i) In the knowledge of the $2mN_c$ canonical Fermi operators $\hat{c}_{n, \mathbf{k}, \sigma}$, and $2N_c(m - 1)$ canonical Fermi operators $\hat{C}_{\alpha, \mathbf{k}, \sigma}$, the remaining $2N_c$ canonical Fermi operators $\hat{C}_{\alpha=m, \mathbf{k}, \sigma}$ can be constructed. ii) Since the complete set of canonical Fermi operators $\hat{C}_{\alpha, \mathbf{k}, \sigma}$, $\alpha = 1, 2, \dots, m$, has been obtained by a linear transformation from the complete set of canonical Fermi operators $\hat{c}_{n, \mathbf{k}, \sigma}$, $n = 1, 2, \dots, m$, the total particle number conservation holds and can be written as

$$\sum_{\mathbf{k}, \sigma} \sum_{n=1}^m \hat{c}_{n, \mathbf{k}, \sigma}^{\dagger} \hat{c}_{n, \mathbf{k}, \sigma} = \sum_{\mathbf{k}, \sigma} \sum_{\alpha=1}^m \hat{C}_{\alpha, \mathbf{k}, \sigma}^{\dagger} \hat{C}_{\alpha, \mathbf{k}, \sigma} = N. \quad (22)$$

iii) Since originates from \hat{H} , \hat{H}_{kin} from (21) must describe m bands, but in (21) only $m - 1$ bands are present. The m th band however can be simply introduced in (21) by taking a constant $b \geq 0$, multiplying (22) by b , adding $bN - bN$ to (21) and introducing the notations $\xi_{\alpha < m}(\mathbf{k}, b) = \eta_{\alpha < m}(\mathbf{k}) + b$, $\xi_{\alpha=m}(\mathbf{k}, b) = +b = const.$, $C_b = -bN$, based on which, (21) becomes

$$\hat{H}_{kin} = \sum_{\mathbf{k}, \sigma} \sum_{\alpha=1}^m \xi_{\alpha}(\mathbf{k}, b) \hat{C}_{\alpha, \mathbf{k}, \sigma}^{\dagger} \hat{C}_{\alpha, \mathbf{k}, \sigma} + C_b. \quad (23)$$

Eq.(23) provides m bands, described by the canonical Fermi operators $\hat{C}_{\alpha, \mathbf{k}, \sigma}^{\dagger}$, while $\xi_{\alpha}(\mathbf{k})$ $\alpha = 1, 2, \dots, m$, is the dispersion relation for the α th band, and C_b is a \mathbf{k} independent constant which globally shifts the energies. As seen from (23), given by $\eta_{\alpha}(\mathbf{k}) < 0$ as shown below (20), $\xi_{\alpha=m}(\mathbf{k}) = b = const.$ is the upper band, and it is flat.

I further underline that based on (17), the emergence of the effective upper flat band, from mathematical point of view can be interpreted as a renormalization of the bare ϵ_n to $\epsilon_n^R = \epsilon_n + U_n - q_U$, where q_U is a nonlinear function of all U_n .

As shown above, the interaction created effective upper flat band emerges on an extremely broad class of polymers. I further note that the effect exceeds the polymer frame, and appears also in higher dimensions (see for example Fig.2 of Ref.^[43]).

V. THE GROUND STATE WAVE FUNCTION

The ground state wave function corresponding to the Hamiltonian presented in (5) for $N = N^*$ number of electrons has the form

$$|\Psi_g(N^*)\rangle = [\prod_{\sigma} \prod_{\mathbf{i}} \prod_{\alpha=1}^{m-1} \hat{G}_{\alpha,\mathbf{i},\sigma}^{\dagger}] \hat{F}^{\dagger} |0\rangle, \quad (24)$$

where $N = N^* = (2m-1)N_c$ (i.e. upper band half filled), $|0\rangle$ is the bare vacuum, and the \hat{F}^{\dagger} operator introduces one electron with fixed spin σ in each unit cells in an arbitrary position (i.e. $\hat{F}^{\dagger} = \prod_{\mathbf{i}} \hat{c}_{\mathbf{i}+\mathbf{r}_i,\sigma}^{\dagger}$, where $\mathbf{i} + \mathbf{r}_i$ represents an arbitrary site in the unit cell placed at the lattice site \mathbf{i} , and σ is fixed). The $N = N^*$ expression emerges because one $\hat{G}_{\alpha,\mathbf{i},\sigma}^{\dagger}$ operator introduces one electron in the system, one has $2N_c(m-1)$ such operators in (24), while \hat{F}^{\dagger} creates N_c electrons, hence $N^* = 2N_c(m-1) + N_c$. The concentration corresponding to (24) is $n_c = N^*/(2N_{\Lambda}) = (2m-1)/(2m)$.

Eq.(24) represents the ground state for the following reasons: i) $\hat{G}_{\alpha,\mathbf{i},\sigma}^{\dagger} \hat{G}_{\alpha,\mathbf{i},\sigma}^{\dagger} = 0$, because the square of an arbitrary linear combination of fermionic operators is always zero. Consequently, since $\hat{G}_{\alpha,\mathbf{i},\sigma}^{\dagger}$ appears both in (3) and (24), it results that $\hat{P}_I |\Psi_g\rangle = 0$. ii) Since at fixed σ , the operator $[\prod_{\mathbf{i}} \prod_{\alpha=1}^{m-1} \hat{G}_{\alpha,\mathbf{i},\sigma}^{\dagger}] \hat{F}^{\dagger}$ introduces $N_{\Lambda} = mN_c$ electrons in the system, one has on each site one electron with spin σ present. Consequently, in $|\Psi_g\rangle$, on all sites of the system one has at least one electron, and as a consequence $\hat{P}_{II} |\Psi_g\rangle = 0$ is also satisfied (see the description of the \hat{P}_I in Sect.I.). In conclusion, $|\Psi_g\rangle$ is the ground state, and the corresponding ground state energy is $E_g = C_g$, where C_g is given below (5). The uniqueness of the solution can be demonstrated on the line of the uniqueness proof from Ref.¹⁶.

I further note that the ground state can be defined also for $N > N^*$. In this case the ground state expression from (24) acquires in its right side a supplementary product of the form $\hat{O}^{\dagger} = \prod_{\gamma=1}^{N-N^*} c_{n,\mathbf{k}_{\gamma},\sigma}^{\dagger}$, where a given, although arbitrary \mathbf{k}_{γ} , appears in \hat{O}^{\dagger} only once. Since plane wave contributions with fixed spin projection are present in \hat{O}^{\dagger} , the ground state at $N > N^*$ becomes a half metallic conducting state.

VI. CHARACTERISTICS OF THE TRANSITION TO THE ORDERED STATE

The obtained ground state represents a non-saturated ferromagnet. In order to understand the reasons of the emergence of this state, for fixed Hamiltonian parameters placed

inside \mathcal{D} , one calculates in the presence of the interaction terms different energies (as kinetic energy, interaction energy and total energy) using first the non-interacting ground state $|\Psi_{0,g}\rangle$ as a trial state, deducing with it $E_{0,kin}, E_{0,int}, E_{0,g} = E_{0,kin} + E_{0,int}$. Then, in a second step, for the same Hamiltonian parameters, one uses $|\Psi_g\rangle$ from (24) in order to deduce the exact E_{kin}, E_{int}, E_g . Calculating the relative deviations via $\delta E_{kin} = (E_{kin} - E_{0,kin})/E_{0,kin}$, $\delta E_{int} = (E_{int} - E_{0,int})/E_{0,int}$, and $\delta E_g = (E_g - E_{0,g})/E_{0,g}$, expressing these values in percents, we can analyze how different energy contributions vary when the ordered state (24) emerges. The study has been made on the smallest unit which produces in the presented conditions ferromagnetism, namely the two cell system taken with periodic boundary conditions.

The obtained results are quite interesting and show that above a given degree of complexity of the chain situated above a simple triangular chain case ($m = 2, m_p = 2, m_e = 0$, see Ref.¹⁶), when the ordered state emerges, δE_{kin} is almost zero (the kinetic energy increases 2-3%), the interaction energy strongly decreases (the decrease in δE_{int} often reaches almost 70%), and as a consequence of these variations, the total energy, described by δE_g , decreases 1-2%. As it can be seen, the transition to the ordered phase is clearly driven by the strong decrease of the interaction energy. In the same time, the kinetic energy is practically quenched at (or in the close vicinity of) $E_{0,kin}$, i.e. the kinetic energy present before the interactions have been turned on. These effects appear when differences are present in the Hubbard interactions at different type of sites inside the unit cell, and the behavior disappears when the on-site Coulomb repulsion is homogeneous, i.e. $U_n = U$ for all $n = 1, 2, \dots, m$.

This behavior can be understood by taking into account that in the studied case the on-site Coulomb repulsion values are different on different type of sites. Indeed, in these conditions a supplementary degree of freedom is present for the decrease of the interaction energy, which is completely missing when the Hubbard interaction is homogeneous. Namely, the system can reorganize the local double occupancy d_n such to introduce small d_n where U_n is high and vice verse, obtaining a huge interaction energy decrease relative to the interaction energy values fixed by the double occupancies created by $|\Psi_{0,g}\rangle$.

In order to exemplify, I present in Fig.3 results deduced for the $m = 6$ case plotted in Fig.2.a inside of its \mathcal{D} region⁴⁷ holding in average (in $t = t_{3,4}$ units) $\langle U \rangle = 0.186$ inside the unit cell. Let us consider that one modifies the local Coulomb repulsion values relative to $\langle U \rangle$ as presented in Fig.3.a and calculates the variations in the local average double occupancy created by (24) relative to those double occupancy values, which were fixed by the non-

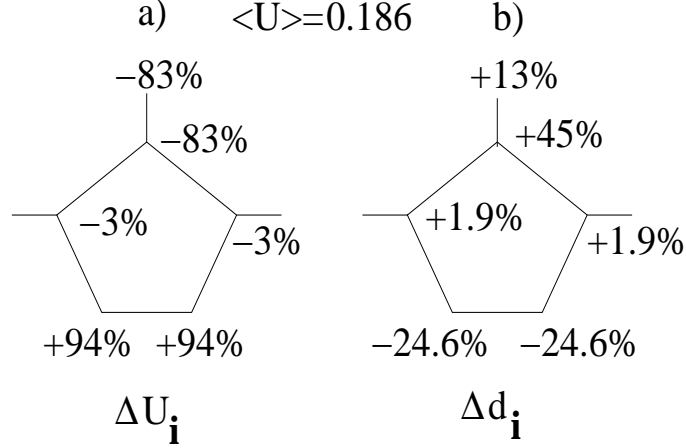


FIG. 3. The modifications Δd_i in the average local double occupancy $d_i = \langle \hat{n}_{i,\uparrow} n_{i,\downarrow} \rangle$ created by the interacting ground state $|\Psi_g\rangle$ in (24) relative to the local double occupancy introduced by the non-interacting ground state $|\Psi_{0,g}\rangle$ (see b)), in function of the local on-site Coulomb repulsion variations $\Delta U_i = U_i - \langle U \rangle$ on different sites (see a)), at $\langle U \rangle = 0.186$ in the case of the exemplified chain in Fig.2.a⁴⁷.

ordered ground state $|\Psi_{0,g}\rangle$. The results are presented in Fig.3.b. As can be seen, on the sites where strong U increase is present (i.e. the local Hubbard interaction is high), the local double occupancy in the interacting and ordered ground state strongly decreases (the two bottom sites where in d_i , 24.6% decrease is observed). Contrary to this, on the sites where the Coulomb repulsion values decrease relative to the average (hence the local Hubbard interaction is small), 45% increase in the double occupancy is observed on the internal site, and a smaller increase, but still high (i.e. 13%, see the top site) is observed in d_i on the external site. On the sites where U_i remains close to the average value (in the present case the sites along the line of the chain), the double occupancy remains almost unchanged (i.e. $\Delta U = -3\%$ produces a $\Delta d_i = +1.9\%$). I note that given by these modifications introduced by the interacting ground state, the interaction energy decreases almost 70 % in the transition from $|\Psi_{0,g}\rangle$ to $|\Psi_g\rangle$, while the kinetic energy increases around 2% in the same process (i.e. remains practically unchanged, quenched).

As can be seen, at the emergence of the ordered phase, the system quenches the kinetic energy, exactly in order to have the possibility to take fully into account the huge interaction energy decrease possibility, which is offered by the non-homogeneous U values inside the unit cell. This kinetic energy quench is the physical reason of the emergence of an interaction

created effective flat band described in the previous section.

I underline that when $U_n = U$ is homogeneous, the redistribution of double occupancy is no more possible, and the here described mechanism completely disappears. I further note that the presented mechanism for the emergence of ferromagnetism is completely different from the Mielke-Tasaki¹⁴ type of flat band ferromagnetism because in the here described case bare flat bands are not present and inhomogeneous U_n values are needed. Furthermore, the properties of the ordered phase are different: for example the conditions leading to \mathcal{D} described at the end of Sect.III provide lower non-zero limits in U_n for the emergence of ferromagnetism.

VII. SUMMARY AND CONCLUSIONS

The technique used in obtaining the results allows to deduce particle number dependent ground states for interacting quantum mechanical many-body systems independent on dimensionality and integrability, and also to obtain non-approximated information relating the low lying part of the excitation spectrum. The procedure is based on positive semidefinite operator properties and uses successively the following steps: a) transforms the Hamiltonian in a positive semidefinite form $\hat{H} = \hat{P} + C_g$ where \hat{P} is a positive semidefinite operator and C_g is a scalar, b) deduces the ground state $|\Psi_g\rangle$ by constructing the most general solution of the equation $\hat{P}|\Psi_g\rangle = 0$. If this equation presents solutions, the corresponding ground state energy becomes $E_g = C_g$. c) demonstrates the uniqueness of the solution, and d) analyzes the physical properties of the deduced phase by calculating elevated ground state expectation values. The procedure, in principle, can be applied always, not requiring *a priori* information relating the ground state wave function or ground state energy.

Based on the presented method, in the high concentration region, a general conducting polymer is analyzed, which represents a non-integrable system, has $m = m_p + m_e > 2$ sites per unit cell, where m_p sites are included in a closed polygon, and m_e sites, representing side groups, are placed outside of it. For the description a Hubbard type of model is used such that different on-site Coulomb repulsion values are allowed at different type of sites inside the unit cell, and the system not possesses bare flat bands. In this conditions, it is rigorously demonstrated that a parameter space region (\mathcal{D}) exists where the interactions create an effective upper flat band.

The deduced ground state wave function in \mathcal{D} , in the present case, turns out to be a non-saturated ferromagnet. The study of the emergence of the ordered phase demonstrates that the transition is entirely driven by a huge decrease of the interaction energy, while in the same time, the kinetic energy is quenched. The kinetic energy quench is the physical reason which produces the effective flat band. This effect requires a given degree of complexity for the chain, and disappears when the Hubbard repulsion becomes homogeneous. The deduced ferromagnetic state i) appears in the presence of dispersive bare bands, but demands an interaction created flat band, ii) requires different on-site Coulomb repulsion values on different type of sites inside the unit cell, iii) leads to non-zero lower limits for the interaction at the emergence of the ordered phase, consequently is completely different from the known flat-band ferromagnetism.

VIII. ACKNOWLEDGMENTS

The author kindly acknowledges financial support provided by Alexander von Humboldt Foundation, OTKA-K-100288 (Hungarian Research Funds for Basic Research) and TAMOP 4.2.2/A-11/1/KONV-2012-0036 (co-financed by EU and European Social Fund).

-
- ¹ W. Kohn, Rev. Mod. Phys. **71**, 1253 (1998).
 - ² V.I. Anisimov, F. Aryasetianwan and A. I. Lichtenstein, Jour. Phys: Condens. Matter **9**, 767 (1997).
 - ³ F. Aryasetianwan and O. Gunnarsson, Rep. Prog. Phys. **61**, 237 (1998).
 - ⁴ W. Metzner and D. Vollhardt, Phys. Rev. Lett. **62**, 324 (1989).
 - ⁵ A. Georges, G. Kotliar, W. Krauth, and M. J. Rozenberg, Rev. Mod. Phys. **68**, 13 (1996).
 - ⁶ M. Städele and R. M. Martin, Phys. Rev. Lett. **84**, 6070 (2000).
 - ⁷ E. H. Lieb and F. Y. Wu, Phys. Rev. Lett. **20**, 1445 (1968).
 - ⁸ Y. Zhang, Y. W. Tan, H. L. Stormer, and P. Kim, Nature **438**, 201 (2005).
 - ⁹ M. Z. Hasan and C. L. Kane, Rev. Mod. Phys. **82**, 3045 (2010).
 - ¹⁰ R. Takahashi and S. Murakami, Phys. Rev. B **88**, 235303 (2013).
 - ¹¹ G. Möller and N. R. Cooper, Phys. Rev. Lett. **108**, 045306 (2012)

- ¹² O. Derzhko, J. Richter, A. Honecker, and R. Moessner, Phys. Rev. B **81**, 014421 (2010).
- ¹³ Z. Gulácsi, Phys. Rev. B **77**, 245113 (2008).
- ¹⁴ A. Mielke and H. Tasaki, Commun. Math. Phys. **158**, 341 (1993).
- ¹⁵ Z. Gulácsi, A. Kampf and D. Vollhardt, Phys. Rev. Lett. **105**, 266403 (2010).
- ¹⁶ Z. Gulácsi, Int. Jour. Mod. Phys. B **27**, 1330009 (2013).
- ¹⁷ A. S. Dhoot, *et al.*, Phys. Rev. Lett. **96**, 246403 (2006).
- ¹⁸ A. C. R. Grayson, *et al.*, Nature Mater. **2**, 767 (2003).
- ¹⁹ R. McNeill, *et al.*, Australian Jour. Chem. **16**, 1056 (1963).
- ²⁰ J. W. van der Horst, P. a. Bobbert and M. A. J. Michels, Phys. Rev. Lett. **83**, 4413 (1999).
- ²¹ O. R. Nascimento, *et al.*, Phys. Rev. B **67**, 14422 (2003).
- ²² F. R. de Paula, *et al.*, Jour. Magn. Magn. Matter. **320**, 193 (2008).
- ²³ A. A. Correa, *et al.*, Synth. Met. **121**, 1836 (2001).
- ²⁴ A. J. Heeger *et al.* Rev. Mod. Phys. **60**, 781 (1988).
- ²⁵ T. O. Wehling, *et al.*, Phys. Rev. Lett. **106**, 236805 (2011).
- ²⁶ G. Brocks, J. Van den Brink and A. F. Morpurgo, Phys. Rev. Lett. **93**, 146405 (2004).
- ²⁷ Y. Suwa, *et al.*, Phys. Rev. B **68**, 174419 (2003).
- ²⁸ R. Arita, *et al.*, Phys. Rev. Lett. **88**, 127202 (2002).
- ²⁹ R. Arita, *et al.*, Phys. Rev. B **68**, 140403(R) (2003).
- ³⁰ Z. Gulácsi and M. Gulacsi, Phys. Rev. Lett. **73**, 3239 (1994).
- ³¹ R. Trencsényi, E. Kovács and Z. Gulácsi, Phil. Mag. **89**, 1953 (2009).
- ³² R. Trencsényi and Z. Gulácsi, Phil. Mag. **92**, 4657 (2012).
- ³³ R. Trencsényi, K. Gulácsi, E. Kovács, and Z. Gulácsi, Ann. Phys. (Berlin) **523**, 741 (2011).
- ³⁴ R. Trencsényi and Z. Gulácsi, Eur. Phys. Jour. B **75**, 511 (2010).
- ³⁵ M. Gulacsi, H. Van Beijeren and A.C. Levi, Phys. Rev. E **47**, 2473 (1993); M. Gulacsi, Phil. Mag. B **76**, 731 (1997).
- ³⁶ M. Gulacsi and R. Chan, J. Supercond **14**, 651 (2001); R. Chan and M. Gulacsi, Phil. Mag. Lett. **81**, 673 (2001); R. Chan and M. Gulacsi, Phil. Mag **84**, 1265 (2004).
- ³⁷ D. J. Scalapino, Rev. Mod. Phys. **84**, 1383 (2012).
- ³⁸ Z. Gulácsi and D. Vollhardt, Phys. Rev. Lett. **91**, 186401 (2003).
- ³⁹ Z. Gulácsi and D. Vollhardt, Phys. Rev. B **72**, 075130 (2005).
- ⁴⁰ Z. Gulácsi, A. Kampf and D. Vollhardt, Phys. Rev. Lett. **99**, 026404 (2007).

- ⁴¹ Z. Gulácsi, A. Kampf and D. Vollhardt, *Progr. Theor. Phys. Suppl.* **176**, 1 (2008).
- ⁴² I. Orlik and Z. Gulácsi, *Phil. Mag. Lett.* **78**, 177 (1998); Z. Gulácsi and I. Orlik, *Jour. of Phys. A* **34**, L359 (2001).
- ⁴³ P. Gurin and Z. Gulácsi, *Phys. Rev. B* **64**, 045118 (2001); Z. Gulácsi, *Eur. Phys. Jour. B* **30**, 295 (2002); Z. Gulácsi, *Phys. Rev. B* **66**, 165109 (2002).
- ⁴⁴ Z. Gulácsi, *Phys. Rev. B* **69**, 054204 (2004).
- ⁴⁵ Z. Gulácsi and M. Gulacsi, *Phys. Rev. B* **73**, 014524 (2006).
- ⁴⁶ As shown in Ref. 16, in the simple triangular case, solutions for $\hat{G}_{\alpha,\mathbf{i},\sigma}^\dagger$ exist, but not are U_n dependent. Furthermore, the $|\delta E_{int}|$ and $|\delta E_{kin}|$ variations are of the same order of magnitude. That is why, a given degree of complexity is needed for the chain in order to provide the described mechanism.
- ⁴⁷ One has in the presented case $t = t_{3,4} = t_{4,5} = t_{5,1} = t_{1,2} = 1$, $t_{6,5} = 1.2$, $t_{2,3} = -1.1$, $t_{i+a,4} = 0.5$, $\epsilon_1 = \epsilon_4 = -2.5$, $\epsilon_2 = \epsilon_3 = -2.0$, $\epsilon_5 = \epsilon_6 = -2.1$, and U_n values expressed in t units.